J Mater Sci: Mater Electron (2013) 24:776–783
DOI 10.1007/s10854-012-0809-3

Influence of diffusion-annealing temperature on physical and mechanical properties of Cu-diffused bulk MgB_2 superconductor

M. Dogruer · Y. Zalaoglu · O. Gorur · O. Ozturk · G. Yildirim · A. Varilci · E. Yucel · C. Terzioglu

Received: 8 May 2012 / Accepted: 19 June 2012 / Published online: 13 July 2012

Abstract This study reports not only the effect of Cu diffusion on physical and mechanical properties of bulk MgB_2 superconductors with the aid of Vickers microhardness (H_v) measurements but also the diffusion coefficient and the activation energy of copper (Cu) in the MgB_2 system using the resistivity measurements for the first time. Cu diffusion is examined over the different annealing temperature such as 650, 700, 750, 800 and 850 °C via the successive removal of thin layers and resistivity measurement of the sample. Further, Vickers microhardness, elastic modulus, yield strength, fracture toughness and brittleness index values of the samples studied are evaluated from microhardness measurements. It is found that all the results obtained depend strongly on the diffusion annealing temperature and applied load. The microhardness values increase with ascending the annealing temperature up to 850 °C owing to the increment in the strength of the bonds between grains but decreasing with the enhancement in the applied load due to Indentation Size Effect behaviour of the bulk samples. Moreover, the diffusion coefficient is observed to enhance from 2.84×10^{-8} to 3.22×10^{-7} cm^2 s^{-1} with the increase of the diffusion-annealing temperature, confirming that the Cu diffusion is more dominant at higher temperatures compared to lower ones. Besides, temperature dependence of the Cu diffusion coefficient is described by the Arrhenius relation $D = 2.66 \times 10^{-3} \exp(-1.09 \pm 0.05\ eV/k_BT)$ and the related activation energy of the Cu ions in the MgB_2 system is obtained to be about 1.09 eV. Based on the relatively low value of activation energy, the migration of the Cu ions primarily proceeds through defects such as pore surfaces and grain boundaries in the polycrystalline structure, resulting in the improvement of the physical and mechanical properties of the bulk MgB_2 samples.

1 Introduction

Since the discovery of the superconductivity, many researchers have endeavored to improve the superconducting, physical, electrical mechanical, structural and flux pinning properties of the superconductor materials to make them suitable for high temperature and magnetic field applications [1–6]. Among the superconductor materials, Magnesium diboride (MgB_2) being a simple binary superconductor at 39 K plays an important role on both the fundamental research and applications in technology and industry because of its remarkable low cost preparation, simple chemical composition, simple crystal structure, low density (2.55 g/cm^3), light weight, high T_c value, low resistivity near T_c (0.4–16 μΩ cm at 40 K), large irreversibility field high upper critical field (14–39 T with $\mu_0 H//ab$),

M. Dogruer · Y. Zalaoglu · O. Gorur · G. Yildirim · A. Varilci · C. Terzioglu (✉)
Department of Physics, Abant Izzet Baysal University, Bolu 14280, Turkey
e-mail: terzioglu_c@ibu.edu.tr

Y. Zalaoglu
Department of Physics, Osmaniye Korkut Ata University, Osmaniye 80000, Turkey

O. Ozturk
Department of Physics, Kastamonu University, Kastamonu 37100, Turkey

E. Yucel
Department of Physics, Mustafa Kemal University, Hatay 31034, Turkey

high intrinsic critical current density ($J_c > 10^7 A/cm^2$), large coherence length, low anisotropy (5.4 at low temperature) values and especially absence of weak-links [7–12]. Hence, the MgB_2 material is a good candidate for theoretical studies and practical applications [13, 14]. The physical and mechanical properties such as the hardness, elastic modulus, yield strength, fracture toughness, brittleness index and ductility are also important parameters for industrial applications of the MgB_2 superconducting samples in the form of single crystal, wire, bulk, thin film, and tapes [15–18]. Indentation microhardness measurements are convenient method to determine the physical and mechanical properties of the samples studied.

According to the literature research, no detailed work has been published on the diffusion coefficient and activation energy of Cu in bulk MgB_2 samples except for our recent work on calculations of the diffusion coefficient and activation energy by means of the lattice parameter *c* in the Cu-diffused bulk MgB_2 samples [19]. In that work, not only the effect of Cu diffusion on the microstructural and superconducting properties of bulk MgB_2 superconductors was investigated but the diffusion coefficient and the activation energy of Cu in MgB_2 system were also determined. The investigations showed that the Cu-diffusion and diffusion-annealing temperature improved the microstructural and superconducting properties. In recent work [20], the role of Cu diffusion and annealing time on microstructural, superconducting, physical and mechanical properties (Vickers microhardness, elastic modulus, yield strength, fracture toughness and brittleness index) of the MgB_2 superconductor materials was studied and it was found that the microstructural, superconducting and mechanical properties of the bulk MgB_2 superconductors are strongly dependent upon the Cu diffusion and diffusion-annealing time. Here, the microhardness measurements of the Cu-diffused bulk MgB_2 superconductors are performed at different applied loads in the range from 0.245 to 2.940 N at room temperature. Vickers microhardness, elastic modulus, yield strength, fracture toughness and brittleness index of the samples prepared are examined. Furthermore, for the first time the diffusion coefficient and the activation energy of the Cu ions in the bulk MgB_2 superconductor are evaluated from the successive removal of thin layers and the resistivity measurement of the samples. The results obtained point out that the physical and mechanical properties of the samples studied in this work improve with both the presence of the Cu ions in the MgB_2 system and the enhancement in the diffusion-annealing temperature. Temperature dependence of the Cu diffusion coefficient in the range of 650–850 °C is also described by the following relation $D = 2.66 \times 10^{-3} \exp\left[\left((-1.09 \pm 0.10)^{eV}/_{k_B T}\right)\right]$.

2 Experimental details

In previous work [19], we examined the function of the copper diffusion on the microstructural and superconducting properties of the MgB_2 superconducting materials. The sample preparation procedure with the resistivity ($\rho - T$), X-ray diffraction (XRD) and scanning electron microscopy (SEM) measurement results was given in detail elsewhere [19]. Moreover, the diffusion coefficient and activation energy of the Cu in the MgB_2 system were determined using the variation of the lattice parameters evaluated from the XRD patterns for the first time. In the present study, using the same samples, the influence of Cu-diffusion in the MgB_2 system on physical and mechanical properties is analyzed by means of microhardness (H_v) measurements. Some important physical and mechanical properties (Vickers microhardness, elastic modulus, yield strength, fracture toughness and brittleness index) for industrial applications of the superconductor materials are deduced from the microhardness measurements. Furthermore, the diffusion coefficient and activation energy values of the Cu ions in the MgB_2 system are investigated with the aid of the variation of the resistivity values.

Microhardness measurements are performed in air by using a digital microhardness tester (SHIMADZU HVM-2) at room temperature to characterize the physical and mechanical properties of the bulk MgB_2 samples annealed at different temperatures. A rigid Vickers pyramidal indenter with various loads such as 0.245, 0.490, 0.980, 1.960 and 2.940 N is applied for a single loading time of 10 s and the diagonals of indentation are measured with an accuracy of ±0.1 μm. The Vickers microhardness values are determined with an average of 20 readings at different locations of specimen surfaces to obtain reasonable mean values for each applied load. All the results obtained for the Cu-diffused samples are compared with that for the pure sample annealed at 850 °C for 1 h. Measurement data automated using GPIB interfaced by a personal computer are recorded via the Labview computer software. Pure sample is also presented as Cu-0 while the Cu-diffused MgB_2 superconductors produced by various annealing temperature such as 650, 700, 750 800 and 850 °C will hereafter be denoted as Cu-650, Cu-700, Cu-750, Cu-800 and Cu-850, respectively.

3 Result and discussion

3.1 Calculation of diffusion coefficient

Several methods are studied for the calculation of the diffusion parameter in polycrystalline high-T_c superconductors [19, 21]. The most common four methods are:

successive removal of thin layers and (1) the resistivity measurement of the sample, (2) the variation of the lattice parameters evaluated from the XRD patterns, (3) the EDXRF, and (4) the radio tracer method. In previous work [19], we determined the diffusion coefficient and activation energy of copper by using the second method. In the present study, the diffusion coefficients of Cu-diffused bulk MgB_2 superconductor are found at various temperatures ranging from 650 to 850 °C by means of the first method. Namely, the resistivity distributions over the thickness of the samples are obtained with the aid of the successive removal of thin plate-parallel layers and resistivity measurement of the samples at room temperature. It is discussed that the conditions of impurity diffusion from a constant source into a semi-infinite solid can be defined by following equation [22, 23]:

$$N(x,t) = N_0\left[1 - erf\left(\frac{x}{2\sqrt{Dt}}\right)\right] \quad (1)$$

where $erf\left[\frac{x}{2\sqrt{Dt}}\right]$ displays the error function with argument $y = \left[\frac{x}{2\sqrt{Dt}}\right]$

$$erf(y) = \left(\frac{2}{\sqrt{\pi}}\right)\int_0^y erf\left(-y^2\right) \quad (2)$$

where $N_0 = N(0,t)$ is the constant concentration on the surface of the sample, N(x, t) presents the impurity concentration at the distance x from the surface, D refers the diffusion coefficient and t is the diffusion-annealing time. The equations imply that the resistivity (ρ) with thickness of the samples studied is similar to the concentration distribution of the diffused impurity. The variation of resistivity $\Delta\rho/\rho_0$ (ρ_0 denotes the resistivity of the pure region of the sample) as a function of thickness of the samples produced is given in Fig. 1. The solid curve illustrates the calculated concentration profile of the Cu ions in the MgB_2 system. In this study, it is supposed that the conditions of impurity diffusion from a constant source into semi-infinite solid are satisfied by Eq. (1) [24]. Therefore, the experimental data obtained fit well with the theoretical curve, and the diffusion coefficients calculated by using Eq. (1) are found to be about 2.84×10^{-8}, 5.20×10^{-8}, 1.02×10^{-7}, 1.89×10^{-7} and 3.22×10^{-7} $cm^2\ s^{-1}$ for the Cu-0, Cu-650, Cu-700, Cu-750, Cu-800 and Cu-850 samples, respectively. Based on these results obtained, the diffusion at lower temperatures is much less significant than the higher ones, confirming that the Cu diffusion in the bulk MgB_2 superconductor depends strongly on the diffusion-annealing temperature. Further, the mean values of the diffusion coefficients of the Cu ions in MgB_2 material as a function of the annealing temperature are depicted in Fig. 2. It is apparent from the

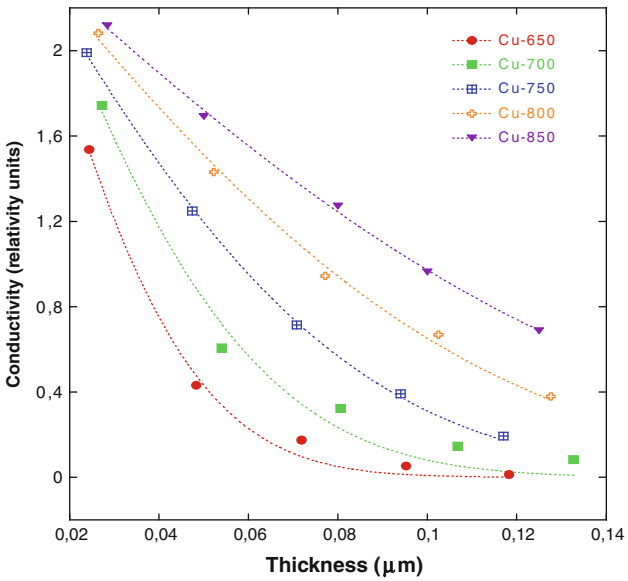

Fig. 1 Variation of the conductivity as a function of sample thickness

figure that the Cu diffusion coefficient in the temperature ranges 650–850 °C increases in terms of the Arrhenius relation,

$$D = 2.66 \times 10^{-3}\exp\left[\left((-1.09 \pm 0.10)^{eV}/_{k_BT}\right)\right] \quad (3)$$

According to the Eq. (3), the activation energy value of the Cu ions in the MgB_2 system is found to be about 1.09 eV, which is in well agreement with a previous work [19]. This relatively low value of activation energy might illustrate that the migration of the Cu primarily proceeds through defects in the polycrystalline sample (pore

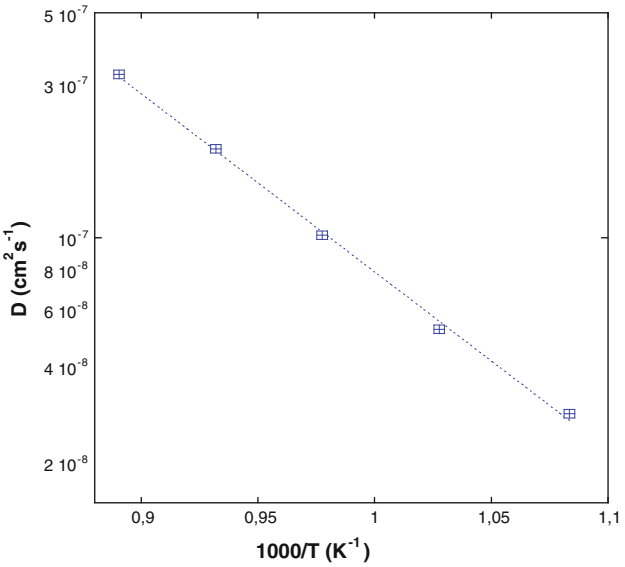

Fig. 2 Temperature dependence of the diffusion coefficient of Cu in the near-surface and inner region of MgB_2

surfaces, grain boundaries, etc.), resulting in the improvement of the physical and mechanical properties of the bulk MgB_2 superconductor. Similar results were reported for Au diffusion in YBaCuO and BSCCO superconductors [25, 26].

3.2 Vickers microhardness measurements

We determine the variation of the diagonal length with regard to the test load to describe the effect of annealing temperature on the physical and mechanical properties of the Cu-diffused bulk MgB_2 samples produced in this work. As well known, the standard Vickers microhardness measurements consist of a load (F) on the test material through geometrically defined indenter and the indenter, removed on the surface of the sample studied, measures the characteristic dimension (d) of the resultant impression.

The Vickers microhardness values at the various applied loads in the range of 0.245–2.940 N are determined using the following equation,

$$H_V = 1854.4\left(\frac{F}{d^2}\right)\ (\mathrm{GPa}) \tag{4}$$

where H_v denotes the Vickers hardness in unit of GPa, F is the applied load in Newton (N) and d presents the mean diagonal length of the indentation impression in unit of μm. The elastic modulus (E), yield strength (Y), fracture toughness (K_{ic}) and brittleness index (B) [27, 28] calculated by means of the following Eqs. (4–8) are summarized in Table 1.

Table 1 The calculated load dependent Hv, E, Y and K_{IC} for the samples

Samples	Load (N)	d (μm)	H_v (GPa)	E (GPa)	Y (GPa)	Kic (Pa/m$^{1/2}$)	B (μm$^{1/2}$)
Cu-0	0.245	14.09	2.288	187.53	0.762	0.750	3.050
	0.490	23.50	1.645	134.83	0.548	0.635	2.590
	0.980	37.04	1.324	108.51	0.441	0.570	2.322
	1.960	62.03	0.944	77.37	0.314	0.481	1.962
	2.940	85.20	0.751	61.55	0.250	0.429	1.750
Cu-650	0.245	13.53	2.481	203.35	0.827	2.316	1.071
	0.490	21.71	1.927	157.94	0.642	2.041	0.944
	0.980	33.07	1.661	136.14	0.553	1.895	0.876
	1.960	51.76	1.356	111.14	0.452	1.712	0.792
	2.940	69.25	1.136	93.11	0.378	1.567	0.724
Cu-700	0.245	12.98	2.696	220.97	0.898	2.424	1.112
	0.490	21.46	1.971	161.55	0.657	2.072	0.951
	0.980	31.64	1.815	148.76	0.605	1.989	0.912
	1.960	49.81	1.464	119.99	0.488	1.786	0.819
	2.940	66.07	1.248	102.29	0.416	1.649	0.756
Cu-750	0.245	11.22	3.608	295.72	1.202	3.027	1.191
	0.490	18.11	2.769	226.95	0.923	2.652	1.044
	0.980	30.06	2.011	164.82	0.670	2.260	0.889
	1.960	44.74	1.815	148.76	0.605	2.147	0.845
	2.940	58.91	1.570	128.68	0.523	1.997	0.786
Cu-800	0.245	10.13	4.427	362.85	1.475	3.481	1.271
	0.490	15.22	3.922	321.46	1.307	3.276	1.197
	0.980	27.21	2.453	201.05	0.817	2.591	0.946
	1.960	40.82	2.181	178.76	0.727	2.443	0.892
	2.940	49.75	2.202	180.48	0.734	2.455	0.896
Cu-850	0.245	9.15	5.423	444.48	1.807	4.310	1.258
	0.490	14.21	4.496	368.50	1.498	3.924	1.145
	0.980	23.39	3.320	272.11	1.106	3.372	0.984
	1.960	38.67	2.429	199.08	0.809	2.884	0.842
	2.940	47.64	2.402	196.87	0.800	2.868	0.837

$$E = 81.9635H_V \quad (5)$$

$$Y \approx \frac{H_V}{3} \quad (6)$$

$$K_{IC} = \sqrt{2E\gamma} \ \ (\gamma, \text{surface energy}) \quad (7)$$

$$B = \frac{H_v}{K_{IC}} \quad (8)$$

Figure 3 displays the variation of microhardness values as a function of applied load for all the superconducting samples. As seen from the table, the microhardness values are sensitively dependent upon the Indentation load (ISE, Indentation Size Effect) and diffusion-annealing temperature. The microhardness value of Cu-0, Cu-650, Cu-700, Cu-750, Cu-800, Cu-850 samples at the constant load of 2.94 N is found to be about 0.751, 1.136, 1.248, 1.570, 2.202 and 2.402 GPa, respectively. Based on the results, the Vickers microhardness values are obtained to increase with both the presence of the Cu ions in the MgB_2 system [19] and the enhancement of the annealing temperature due to the increment in the strength of the bonds between grains.

It is another interesting result from Fig. 3 that although the rapidly decrease in the Vickers microhardness values is obtained with the increase in the applied load from 0.245 to 2.000 N beyond which a slightly change in the microhardness values is observed due to the weakness grain boundaries [29]. In other words, the Vickers microhardness values calculated decrease non-linearly as the applied load increases up to 2 N beyond which the curves measured

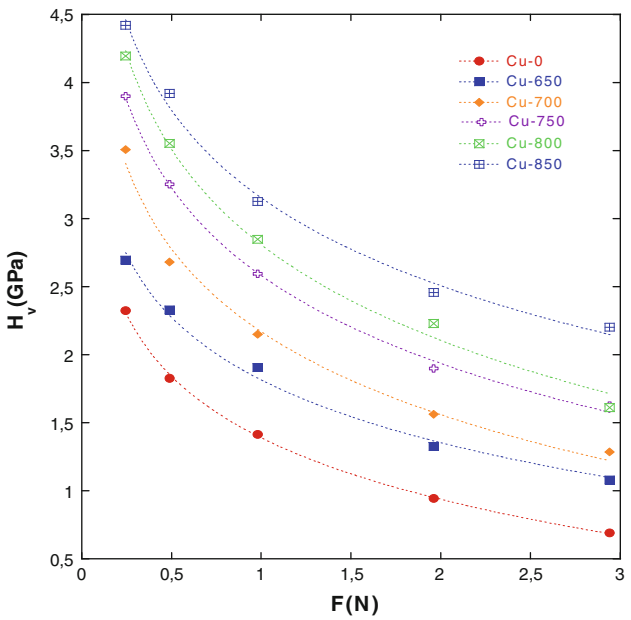

Fig. 3 Variation of microhardness values with applied loads for the samples

shift to the saturation (plateau) region. It is explained that when the applied load is smaller enough, the indenter affects only surface layers and thus the surface effect becomes dominant. On the other hand, when the applied load is higher, the penetration depth enhances and the effect of inner layers appears as more prominent. Hence, no change in the microhardness values is observed with the applied load [30]. This non-linearity has also been observed in the literature for BSCCO samples [31–33] and MgB_2 samples [34, 35], and it is known as indentation size effect (ISE) [36–41].

Moreover, the elastic modulus (E), yield strength (Y), fracture toughness (K_{ic}) and brittleness index (B) values inferred from the Vickers microhardness measurements are found to increase with ascending the diffusion-annealing temperature up to 850 °C while these parameters are observed to decrease with the increment in the applied load, presenting that the E, Y, K_{ic} and B values obtained are strongly dependent upon the applied load. Table 1 indicates that the load dependent E, Y and K_{IC} enhance with the decrement in the applied loads as a result of the crack initiation of microhardness [42–44]. As well known, a change in E, Y and K_{ic} values is attributed to a change in the average surface energy as proposed from the hardness calculations [45].

The load dependence is expressed by two different methods [46]: the elastic portion and energy dissipative process. In the former method, it is assumed that the indentation contains an elastic portion. The elastic part of the deformation is relaxed upon unloading. It can be accounted for by adding an elastic component (d_e) to the measured plastic indentation semidiagonal (d_p). Hence, the true hardness value (H_0) can be defined by means of the following formula [47]:

$$H_0 = 1854.4\left(\frac{F}{(de + dp)^2}\right) \quad (9)$$

The Eq. (9) points out that the indentation diagonals measured should be linear with the square root of the applied load. The slope of such a curve is proportional to $(H_0)^{1/2}$ and the vertical intercept of this graph is proportional to the elastic part of the indentation semidiagonal (d_e). Furthermore, the load dependence of the indentation diagonals for the samples is reanalyzed with the aid of d_p versus $F^{1/2}$ plots, as shown in Fig. 4.

The H_0, d_e and linear regression coefficients (LRC) values extracted from Fig. 4 for all samples are listed in Table 2. It is obvious that such plots are linear with the estimated LRC better than 99.9 %, implying that the Eq. (9) provides a satisfactory description to calculate the true hardness of the indentation data for the samples. As seen from the table, while the H_0 values of the samples

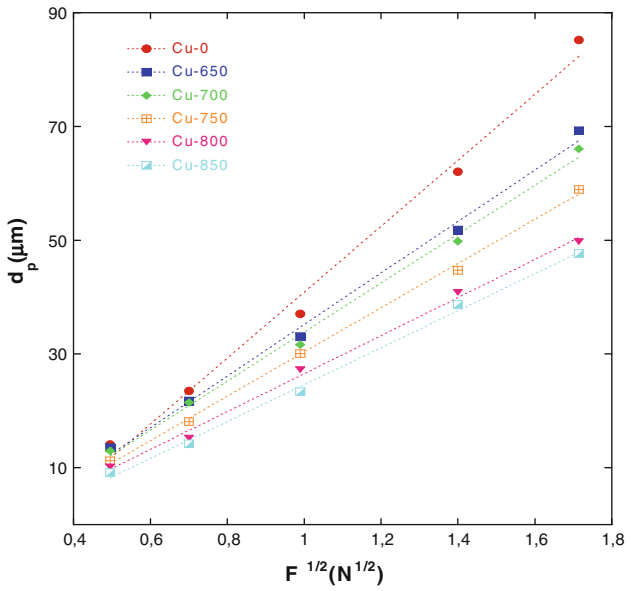

Fig. 4 Graph of diagonal length versus square root of applied loads for the samples prepared

studied increase slightly, the d_e values change randomly with the increment diffusion-annealing temperature. The maximum (minimum) d_e value is observed for the Cu-0 (Cu-800) sample. Additionally, it is indicated in literature that the hardness–load curve exhibits distinct transition (related to the intrinsic hardness value of the material) to a plateau of constant hardness [48], and the H_0 values are nearly close to the experimentally estimated H_v values in the plateau region [49].

In this study, this plateau is reached at 2 N applied load for all the samples studied. Table 2 demonstrates that the true microhardness value of the Cu-0 sample is lower than the hardness results (Table 1) in the plateau region ($H_v = 0.944$ GPa and 0.751 GPa). Other samples prepared in this work exhibit the same behaviour. However, the true hardness value of the samples is lower than that of the traditionally calculated ones. According to the results, this model (elastic portion) is not suitable for our results obtained because of the difference between the calculated results and true hardness values.

Table 2 Best-fit results of experimental data according to Eq. 9

Samples	H_0 (GPa)	de (μm)	LRC	H_v (GPa)
Cu-0	0.551	0.301	0.99566	0.751–0.944
Cu-650	0.904	0.227	0.99768	1.136–1.356
Cu-700	1.001	0.217	0.99787	1.248–1.464
Cu-750	1.224	0.223	0.99916	1.570–1.815
Cu-800	1.660	0.206	0.99814	2.202–2.181
Cu-850	1.756	0.243	0.99845	2.402–2.429

Additionally, the latter (energy dissipative process) method considering energy dissipative processes rather than elastic processes during the indentation is applied consistently to the measured data [46]. In this method, a true microhardness can be defined by subtracting a dissipative part (F_0) from the applied load. Namely,

$$Hv = 1854.4\left(\frac{F - F_0}{d^2}\right) \tag{10}$$

The variation of the applied load as a function of the square of the impression semidiagonal length for the samples is given in Fig. 5. Each set of data indicates an excellent linear relationship (LRC > 0.99). In this figure, the slope of each line corresponds to the load independent hardness constant (H_0) and the intercept of each line represents the sample resistance pressure (F_0). The extracted values of the F_0, H_0 and LRC are tabulated in Table 3. It is visible form the table, whereas the H_0 values of the samples increase, the F_0 values reduce with the increase in the diffusion-annealing temperature. Moreover, the LRC values of each sample are found to be very high, implying that Eq. (10) gives a satisfactory description of the indentation data for all the samples produced. Besides, the diagonal length is found to be strictly dependent upon the applied load. This expression can be identified with the aid of the following relation [50]:

$$\frac{F}{d} = H_0 d + \gamma \tag{11}$$

Figure 6 illustrates the values of F/d against the diagonal length of indentation (d) for the samples. As seen from the figure, each set of data shows an excellent

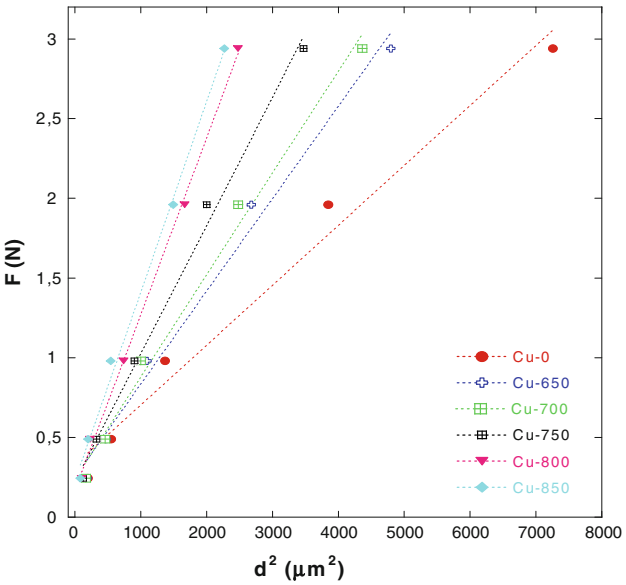

Fig. 5 Variation of applied load with square of diagonal lengths for the samples produced

Table 3 Best-fit results of experimental data according to Eq. 10

Samples	H_0 (GPa)	F_0 (N)	LRC	H_v (GPa)
Cu-0	0.696	0.3289	0.9905	0.751–0.944
Cu-650	1.077	0.2506	0.9944	1.136–1.356
Cu-700	1.185	0.2383	0.9951	1.248–1.464
Cu-750	1.492	0.2234	0.9971	1.570–1.815
Cu-800	2.051	0.1689	0.9991	2.202–2.181
Cu-850	2.208	0.1576	0.9980	2.402–2.429

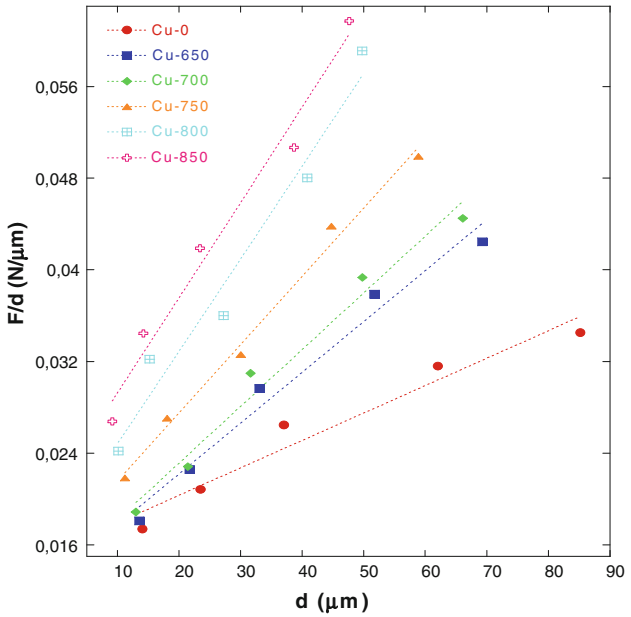

Fig. 6 Plots of F/d versus d for the samples

Table 4 Best-fit results of experimental data according to Eq. 11

Samples	H_0 (GPa)	γ (N/μm)	LRC	H_v (GPa)
Cu-0	0.444	0.0015	0.9749	0.751–0.944
Cu-650	0.822	0.0132	0.9886	1.136–1.356
Cu-700	0.918	0.0133	0.9890	1.248–1.464
Cu-750	1.105	0.0155	0.9958	1.570–1.815
Cu-800	1.498	0.0167	0.9829	2.202–2.181
Cu-850	1.542	0.0209	0.9895	2.402–2.429

linear relationship. The slope of each line corresponds to the true hardness (H_0) and the intercept of each line represents the surface energy (γ). The extracted values of H_0, γ and LRC are summarized in Table 4. It is found that the values of H_0 and γ of all the samples increase slightly with ascending the diffusion-annealing temperature. This observation is interpreted as the dissipation of the energy of cracks at the interfaces [51, 52].

Table 5 The calculated load independent H_0, E_0, Y_0, B_0 and K_{1C} for the samples

Samples	H_0 (GPa)	E_0 (GPa)	Y_0 (GPa)	K_{1C} (Pa/m$^{1/2}$)	B_0 (μm$^{1/2}$)	H_v (GPa)
Cu-0	0.444	36.391	0.148	0.330	1.345	0.751–0.944
Cu-650	0.822	67.374	0.274	1.333	0.616	1.136–1.356
Cu-700	0.918	75.242	0.306	1.414	0.649	1.248–1.464
Cu-750	1.105	90.569	0.368	1.675	0.659	1.570–1.815
Cu-800	1.498	122.781	0.499	2.025	0.739	2.202–2.181
Cu-850	1.542	126.387	0.514	2.298	0.671	2.402–2.429

In addition, the load independent values of elastic modulus (E_0), yield strength (Y_0), brittleness index (B_0) and fracture toughness (K_{ic}) of the samples calculated by means of the true microhardness(load independent, H_0) are given in Table 5. It is apparent from the table that the load independent values of the E_0, Y_0 and K_{ic} are found to enhance with the increment in the diffusion-annealing temperature. On the other hand, the change of the B_0 is randomly found for all the samples. According to the results, the load independent values obtained for the bulk samples are found to be closer to the experimentally estimated values in the plateau region, compared to the load dependent values (Table 1). As a result, the energy dissipation method allows us to investigate the behavior of the samples in the plateau region rather than the elastic portion method, being in excellent agreement with the literature [53, 54]. All in all, the Cu diffusion obtains a positive effect on the mechanical properties of the bulk MgB_2 system.

4 Conclusion

In summary, the physical and mechanical properties of Cu-diffused bulk MgB_2 superconductors prepared at different annealing temperatures such as 650, 700, 750, 800 and 850 °C are investigated by means of Vickers microhardness (H_v) measurements. Further, the diffusion coefficient and activation energy values of the copper ions in the MgB_2 system are clearly reported by the successive removal of thin layers and resistivity measurement of the samples. The results obtained indicate that Vickers microhardness, elastic modulus, yield strength, fracture toughness and brittleness index values deduced from microhardness measurements enhance with the increment in the annealing temperature due to the enhancement in the strength of the bonds between grains; however, the increase in the applied load on the samples causes to degrade these parameters, confirming that the MgB_2 samples prepared in this work exhibit the typical indentation size effect behavior. Additionally, the diffusion coefficient of the Cu in the MgB_2 system in a range of

650–850 °C is determined to increase from 2.84×10^{-8} to 3.22×10^{-7} cm^2 s^{-1} with activation energy of about 1.09 eV, presenting that the Cu diffusion at higher temperatures is much more significant and the Cu ions primarily proceed through the defects in the polycrystalline structure. According to the results, it is concluded that the Cu-diffusion improves the physical and mechanical properties of the bulk MgB_2 superconductor with the increase of the annealing temperature up to 850 °C.

References

1. C.H. Cheng, Y. Yang, C. Ke, H.T. Lin, Phys. C **470**, 1092 (2010)
2. A. Varilci, D. Yegen, M. Tassi, D. Stamopoulos, C. Terzioglu, Phys. B **404**, 4054 (2009)
3. Y. Zhang, S.H. Zhou, X.L. Wang, S.X. Dou, Phys. C **468**, 1383 (2008)
4. C. Terzioglu, A. Varilci, I. Belenli, J. Alloys Comp. **478**, 836 (2009)
5. M. Zongqing, L. Yongchang, S. Qingzhi, Z. Qian, G. Zhiming, J. Alloys Comp. **471**, 105 (2009)
6. Q. Cai, Y. Liu, Z. Ma, Z. Dong, J. Supercond. Novel Magn. (2012). doi:10.1007/s10948-011-13160
7. J. Nagamatsu, N. Nakagawa, T. Muranaka, Y. Zenitani, J. Akimitsu, Nature **410**, 63 (2001)
8. A.A. Golubov, A. Brinkman, O.V. Dolgov, J. Kortus, O. Jepsen, Phys. Rev. B **66**, 054524 (2002)
9. J.D. Fletcher, A. Carrington, O.J. Taylor, S.M. Kazakov, J. Karpinski, Phys. Rev. Lett. **95**, 097005 (2005)
10. M. Zehetmayer, M. Eisterer, J. Jun, S.M. Kazakov, J. Karpinski, A. Wisniewski, H.W. Weber, Phys. C **408**, 111 (2004)
11. M. Angst, D.Di Castro, D.G. Eshchenko, R. Khasanov, S. Kohout, I.M. Savic, A. Shengelaya, S.L. Bud'ko, P.C. Canfield, J. Jun, J. Karpinski, S.M. Kazakov, R.A. Ribeiro, H. Keller, Phys. Rev. B **70**, 224513 (2004)
12. Y. Bugoslavsky, G.K. Perkins, X. Qi, L.F. Cohen, A.D. Caplin, Nature **410**, 563 (2001)
13. K. Vinod, R.G.A. Kumar, U. Syamaprasad, Supercond. Sci. Technol. **20**, R1 (2007)
14. C. Buzea, T. Yamashita, Supercond. Sci. Technol. **14**, R115 (2001)
15. Y. Zhao, M. Ionescu, J. Horvat, S.X. Dou, Supercond. Sci. Technol. **17**, S482 (2004)
16. B. Birajdara, O. Eibl, J. Appl. Phys. **105**, 033903 (2009)
17. Q. Zhao, L. Yongchang, H. Yajing, M. Zongqing, S. Qingzhi, G. Zhiming, Phys. C **469**, 857 (2009)
18. O. Ozturk, M. Erdem, E. Asikuzun, O. Yildiz, G. Yildirim, A. Varilci, C. Terzioglu, J. Mater. Sci.: Mater. Electron. (2012). doi:10.1007/s10854-012-0722-9
19. M. Dogruer, G. Yildirim, E. Yucel, C. Terzioglu, (2012) doi: 10.1007/s10854-012-0689-6
20. M. Dogruer, O. Gorur, Y. Zalaoglu, O. Ozturk, G. Yildirim, A. Varilci, C. Terzioglu, J. Mater. Sci.: Mater. Electron. (2012). doi:10.1007/s10854-012-0755-0
21. C. Terzioglu, H. Aydin, O. Ozturk, E. Bekiroglu, I. Belenli, Phys. B **403**, 3354 (2008)
22. C. Terzioglu, Phys. B **403**, 3320 (2008)
23. C. Terzioglu, O. Ozturk, I. Belenli, J. Alloys Comp. **471**, 142 (2009)
24. G.B. Abdullaev, T.D. Dzhafarov, *Atomic Diffusion in Semiconductor Structures* (Harwood Academic Publishers, Chur, 1987)
25. T.D. Dzhafarov, M. Altunbas, A. Varilci, T. Kucukomeroglu, Mater. Lett. **25**, 81 (1995)
26. O. Ozturk, T. Kucukomeroglu, C. Terzioglu, J. Phys. Condens. Matter **19**, 346205 (2007)
27. O. Ozturk, H.A. Cetinkara, E. Asikuzun, M. Akdogan, M. Yilmazlar, C. Terzioglu, J. Mater. Sci.: Mater. Electron. **22**, 1501 (2011)
28. E. Asikuzun, O. Ozturk, H.A. Cetinkara, G. Yildirim, A. Varilci, M. Yılmazlar, C. Terzioglu, J. Mater. Sci.: Mater. Electron. (2011). doi:10.1007/s10854-011-0537-0
29. H.C. Ling, M.F. Yan, J. Appl. Phys. **64**, 1307 (1988)
30. N.H. Mohammed, A.I. Abou-Aly, I.H. Ibrahim, R. Awad, M. Rekaby, J. Supercond. Novel Magn. **24**, 1463 (2011)
31. M. Yilmazlar, H.A. Cetinkara, M. Nursoy, O. Ozturk, C. Terzioglu, Phys. C **442**, 101 (2006)
32. A. Murakami, K. Katagiri, K. Noto, K. Kasaba, Y. Sohoji, M. Muralidhar, N. Sakai, M. Murakami, Phys. C **794**, 378 (2002)
33. S.M. Khalil, Smart Mater. Struct. **14**, 804 (2005)
34. U. Kolemen, J. Alloys Comp. **425**, 429 (2006)
35. U. Kolemen, O. Uzun, M.A. Aksan, N. Guclu, E. Yakıncı, J. Alloys Comp. **415**, 294 (2006)
36. R. Tickoo, R.P. Tandon, K.K. Bamzai, P.N. Kotru, Mater. Chem. Phys. **80**, 446 (2003)
37. A.A. Elmustafa, D.S. Stone, J. Mech. Phys. Solids **51**, 357 (2003)
38. J. Gong, J. Wu, Z. Guan, Mater. Lett. **38**, 197 (1999)
39. K. Sangwal, B. Surowska, Mater. Res. Innov. **7**, 91 (2003)
40. T.D. Dzhafarov, M. Altunbas, A. Varilci, T. Kucukomeroglu, S. Nezir, Solid State Commun. **99**, 839 (1996)
41. O. Gorur, T. Kucukomeroglu, C. Terzioglu, A. Varilci, M. Altunbas, Phys. C **418**, 35 (2005)
42. A. Goyal, P.D. Funkenbusch, D.M. Kroeger, S.J. Burns, J. Appl. Phys. **71**, 2363 (1992)
43. S.M. Khalil, J. Phys. Chem. Solids **62**, 457 (2001)
44. C. Veerender, V.R. Dumke, M. Nagabhooshanam, Phys. Status Solid A **144**, 299 (1994)
45. O. Ozturk, C. Terzioglu, I. Belenli, J. Supercond. Novel Magn. **24**, 381 (2011)
46. A. Leenders, M. Ullrich, H.C. Freyhardt, Phys. C **279**, 173 (1997)
47. Z. Li, A. Ghosh, A.S. Kobayashi, J. Am. Soc. **72**, 904 (1989)
48. J.B. Quinn, G.D. Quinn, J. Mater. Sci. **31**, 4331 (1997)
49. O. Ozturk, E. Asikuzun, M. Erdem, G. Yildirim, O. Yildiz, C. Terzioglu, J. Mater. Sci.: Mater. Electron. **23**, 511 (2012)
50. K. Hirao, M. Tomozawa, J. Am. Ceram. Soc. **70**, 497 (1987)
51. F. Frohlinch, P. Grau, W. Grellmann, Phys. Status Solidi A **42**, 79 (1977)
52. E.O. Bernhardt, Z. Metall. **33**, 135 (1941)
53. M. Yilmazlar, O. Ozturk, O. Gorur, I. Belenli, C. Terzioglu, Supercond. Sci. Technol. **20**, 365 (2007)
54. F.A. McClintock, A.S. Argon, *Mechanical Behaviour of Materials* (Addison-Wesley, Reading, MA, 1996), p. 455